Comparison between different formulations for the solution of 3D nonlinear magnetostatic problems using BEM-FEM coupling

Joachim Fetzer, Stefan Kurz and Günther Lehner
Institut für Theorie der Elektrotechnik, Universität Stuttgart, Pfaffenwaldring 47, 70550 Stuttgart, Germany

Abstract—Two formulations of the BEM-FEM coupling method for 3D nonlinear magnetostatic problems have been developed. Different ways of introducing the Coulomb gauge and handling of the respective boundary terms are discussed. Several iterative methods for the solution of the discretized equations are presented. An example of the TEAM workshop (Testing Electromagnetic Analysis Methods) has been used to examine the numerical behaviour.

I. Introduction

Fig. 1 shows a typical configuration for the BEM-FEM coupling method. Starting from Maxwell-equations describing magnetostatic problems and taking into account the constitutive relation $\vec{H} = \nu(|\vec{B}|)\vec{B}$ and the magnetic vector potential $\vec{A}$, the equations are

$$\left.\begin{aligned} \operatorname{rot}\nu\operatorname{rot}\vec{A} &= \vec{g}_S \\ \operatorname{div}\vec{A} &= 0 \end{aligned}\right\} \quad \text{in} \quad \Omega\,. \tag{1}$$

$\vec{H}$ is the magnetic field strength, $\vec{B}$ the flux density, ν the reluctivity and $\vec{g}_S$ denotes the source current density. Coulomb gauge is prescribed to ensure uniqueness of $\vec{A}$.

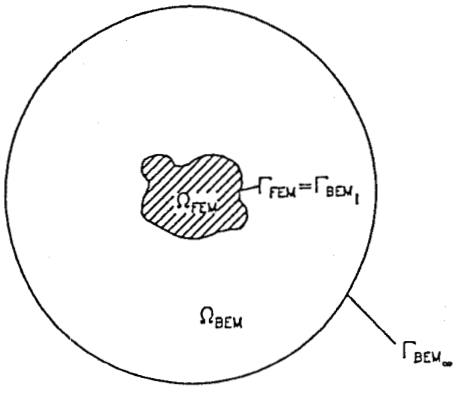

Fig. 1. Structure of the considered domain $\Omega = \Omega_{FEM} \cup \Omega_{BEM}$

Manuscript received July 10, 1995.
J. Fetzer, e-mail joachim.fetzer@rus.uni-stuttgart.de;
S. Kurz, e-mail stefan.kurz@rus.uni-stuttgart.de.

A suitable boundary condition is

$$\vec{A} = \vec{0} \quad \text{on} \quad \Gamma_{BEM\infty}\,. \tag{2}$$

It is assumed that there are no magnetizable bodies in Ω_{BEM} ($\nu = \nu_0$).

II. The first formulation

The first formulation is [1]

$$\operatorname{rot}\nu\operatorname{rot}\vec{A} - \operatorname{grad}\nu\operatorname{div}\vec{A} = \vec{g}_S \quad \text{in} \quad \Omega\,, \tag{3}$$

$$\vec{A} = \vec{0} \quad \text{on} \quad \Gamma_{BEM\infty}\,. \tag{4}$$

Equations (3), (4) have the same unique solution as (1), (2) as long as $\operatorname{div}\vec{g}_S = 0$ holds. The weak integral form is

$$\int_{\Omega_{FEM}} \nu\left(\operatorname{rot}\vec{A}\cdot\operatorname{rot}\vec{w} + \operatorname{div}\vec{A}\operatorname{div}\vec{w}\right)\mathrm{d}\Omega - \oint_{\Gamma_{FEM}} \vec{Q}_1\cdot\vec{w}\,\mathrm{d}\Gamma = \int_{\Omega_{FEM}} \vec{g}_S\cdot\vec{w}\,\mathrm{d}\Omega\,, \tag{5}$$

$$\vec{Q}_1 = \nu\left(\operatorname{rot}\vec{A}\times\vec{n} + (\operatorname{div}\vec{A})\vec{n}\right)\,. \tag{6}$$

A FEM discretization of (5) using C^0-continuous nodal elements ensures the continuity of $\vec{Q}_1$ at the element interfaces. This implies continuity of $\vec{H}_t$ **and continuity of** $\nu\operatorname{div}\vec{A}$. A similar integration by parts taking into account $\nu = \nu_0$ in Ω_{BEM} results in

$$-\nu_0\int_{\Omega_{BEM}}(\vec{\Delta}\vec{w})\cdot\vec{A}\,\mathrm{d}\Omega + \nu_0\oint_{\Gamma_{BEM}}\left(\operatorname{rot}\vec{w}\times\vec{n} + (\operatorname{div}\vec{w})\vec{n}\right)\cdot\vec{A}\,\mathrm{d}\Gamma - \oint_{\Gamma_{BEM}}\vec{Q}_1\cdot\vec{w}\,\mathrm{d}\Gamma = \int_{\Omega_{BEM}}\vec{g}_S\cdot\vec{w}\,\mathrm{d}\Omega\,. \tag{7}$$

The Cartesian components of $\vec{w}$ can successively be chosen as the fundamental solution u^* of the 3D scalar Laplace equation, yielding

$$\nu_0 c\vec{A} + \nu_0\oint_{\Gamma_{BEM}}\left((\vec{n}\times\operatorname{grad}u^*)\times\vec{A} + q^*\vec{A}\right)\mathrm{d}\Gamma - \oint_{\Gamma_{BEM}}\vec{Q}_1 u^*\,\mathrm{d}\Gamma = \int_{\Omega_{BEM}}\vec{g}_S u^*\,\mathrm{d}\Omega\,, \tag{8}$$

$$q^* = \frac{\partial u^*}{\partial n}, \quad c = \text{local edge factor}. \tag{9}$$

Equation (8) is the starting point for the BEM discretization, which can be coupled to (5) using the continuity of $\vec{A}$ and $\vec{Q}_1$ on $\Gamma_{\text{FEM}} = \Gamma_{\text{BEM}}$. However, the BEM formulation developed so far has drawbacks due to the term $(\vec{n} \times \text{grad}\, u^*) \times \vec{A}$ in (8). The Cartesian components of $\vec{A}$ are coupled by this term, which is not the case for all other terms in (8). Moreover, this term involves tangential derivatives of u^*, so that the first integral in (8) exists only in the sense of a Cauchy principal value. Such integrals require special numerical treatment [2]. To avoid possible difficulties, the BEM-FEM-formulation can be modified by defining

$$\vec{Q}_1' = \vec{Q}_1 + \nu_0(\vec{n} \times \text{grad}\,) \times \vec{A}. \tag{10}$$

The additional term $(\vec{n} \times \text{grad}\,) \times \vec{A}$ contains only tangential derivatives of $\vec{A}$, it is continuous on $\Gamma_{\text{FEM}} = \Gamma_{\text{BEM}}$ due to the continuity of $\vec{A}$. As a consequence, continuity of $\vec{Q}_1$ is equivalent to continuity of $\vec{Q}_1'$. Introduction of (10) into (5), (8) and application of the identity

$$\oint_\Gamma (\vec{n} \times \text{grad}\, u) \times \vec{a}\, \text{d}\Gamma + \oint_\Gamma u(\vec{n} \times \text{grad}\,) \times \vec{a}\, \text{d}\Gamma = \vec{0} \tag{11}$$

to (8) results in

$$\int_{\Omega_{\text{FEM}}} \nu \left(\text{rot}\, \vec{A} \cdot \text{rot}\, \vec{w} + \text{div}\, \vec{A}\, \text{div}\, \vec{w} \right) \text{d}\Omega + \nu_0 J(\vec{A}, \vec{w}) - \oint_{\Gamma_{\text{FEM}}} \vec{Q}_1' \cdot \vec{w}\, \text{d}\Gamma = \int_{\Omega_{\text{FEM}}} \vec{g}_{\text{S}} \cdot \vec{w}\, \text{d}\Omega, \tag{12}$$

$$J(\vec{A}, \vec{w}) = \oint_{\Gamma_{\text{FEM}}} \left((\vec{n} \times \text{grad}\,) \times \vec{A} \right) \cdot \vec{w}\, \text{d}\Gamma, \tag{13}$$

$$\nu_0 c \vec{A} + \nu_0 \oint_{\Gamma_{\text{BEM}}} q^* \vec{A}\, \text{d}\Gamma - \oint_{\Gamma_{\text{BEM}}} \vec{Q}_1' u^*\, \text{d}\Gamma = \int_{\Omega_{\text{BEM}}} \vec{g}_{\text{S}} u^*\, \text{d}\Omega. \tag{14}$$

Equation (14) is the BEM formulation of the vector Laplacian. It avoids the disadvantages mentioned above and can be coupled to (12) using the the continuity of $\vec{A}$ and $\vec{Q}_1'$ on the common boundary.

III. The second formulation

The second formulation is obtained by replacing $\nu \text{div}\, \vec{A}$ by $\nu_0 \text{div}\, \vec{A}$ in (3),

$$\text{rot}\, \nu \text{rot}\, \vec{A} - \text{grad}\, \nu_0 \text{div}\, \vec{A} = \vec{g}_{\text{S}} \quad \text{in} \quad \Omega, \tag{15}$$

$$\vec{A} = \vec{0} \quad \text{on} \quad \Gamma_{\text{BEM}\infty} \tag{16}$$

and has still the same solution as (1), (2), provided that $\text{div}\, \vec{g}_{\text{S}} = 0$. The weak integral form can be written down in an analogous way and by introducing the magnetization $\vec{M} = \vec{B} - \vec{H}/\nu_0$ we obtain

$$\nu_0 \int_{\Omega_{\text{FEM}}} \left(\text{rot}\, \vec{A} \cdot \text{rot}\, \vec{w} + \text{div}\, \vec{A}\, \text{div}\, \vec{w} \right) \text{d}\Omega - \nu_0 \int_{\Omega_{\text{FEM}}} \vec{M} \cdot \text{rot}\, \vec{w}\, \text{d}\Omega - \oint_{\Gamma_{\text{FEM}}} \vec{Q}_2 \cdot \vec{w}\, \text{d}\Gamma = \int_{\Omega_{\text{FEM}}} \vec{g}_{\text{S}} \cdot \vec{w}\, \text{d}\Omega, \tag{17}$$

$$\vec{Q}_2 = \nu \text{rot}\, \vec{A} \times \vec{n} + \nu_0 (\text{div}\, \vec{A}) \vec{n}. \tag{18}$$

It is interesting to compare (17) with the identity

$$\int_\Omega \left(\text{rot}\, \vec{a} \cdot \text{rot}\, \vec{b} + \text{div}\, \vec{a}\, \text{div}\, \vec{b} \right) \text{d}\Omega = \int_\Omega \sum_{i=1}^{3} \text{grad}\, a_i \cdot \text{grad}\, b_i\, \text{d}\Omega - J(\vec{a}, \vec{b}), \tag{19}$$

where a_i, b_i are the Cartesian components of $\vec{a}, \vec{b}$ and $J(\vec{a}, \vec{b})$ is defined in (13). The first integral in (17) differs from the weak form of the vector Laplacian only by the boundary integral J. It is important to note that the continuity of $\vec{A}$ and $\vec{w}$ is sufficient to guarantee continuity of J. For this reason, all the coefficients due to J in the FEM element matrices cancel automatically during assembly of the first integral in (17) [3]. The same considerations are valid for (12) in case of $\nu = \nu_0$. From (17) we obtain by using (19) after some calculations

$$\nu_0 \int_{\Omega_{\text{FEM}}} (\text{grad}\, w \cdot \text{grad}\,) \vec{A}\, \text{d}\Omega - \nu_0 \int_{\Omega_{\text{FEM}}} \vec{M} \times \text{grad}\, w\, \text{d}\Omega - \oint_{\Gamma_{\text{FEM}}} \vec{Q}_2' w\, \text{d}\Gamma = \int_{\Omega_{\text{FEM}}} \vec{g}_{\text{S}} w\, \text{d}\Omega, \tag{20}$$

$$\vec{Q}_2' = \vec{Q}_2 + \nu_0 (\vec{n} \times \text{grad}\,) \times \vec{A} \tag{21}$$

$$= \nu_0 \left((\vec{n} \cdot \text{grad}\,) \vec{A} - \vec{M} \times \vec{n} \right). \tag{22}$$

In contrast to the previous section, continuity of $\vec{Q}_2'$ and therefore continuity of $\vec{H}_t$ **and continuity of $\nu_0 \text{div}\, \vec{A}$** is guaranteed by the FEM discretization. The BEM formulation (14) is suitable to be coupled with (20), because in Ω_{BEM} we have $\nu = \nu_0$ and therefore $\vec{Q}_1' = \vec{Q}_2'$.

IV. Iterative Solution

The solution of (12), (14) or (20), (14), respectively, must be obtained by iteration in case of nonlinear media. The basic idea is always to replace the nonlinear problem by a sequence of linear problems. The different iterative methods can be classified by their iteration matrix [4]:

- The tangential matrix leads to the Newton-Raphson method. This can be interpreted as replacing the nonlinear problem by a series of linear but anisotropic problems [5].

- The stiffness matrix of the linear problem defined by the values of ν from the previous step leads to the $\nu(B)$-iteration [5], [6].
- The stiffness matrix of the vacuum problem ($\nu = \nu_0$, $\vec{M} = \vec{0}$) leads to a $M(B)$-iteration [4], [5], [7].

The $M(B)$-method is especially effective concerning its memory requirements. The vacuum stiffness matrices of the formulations (12) and (20) are completely decoupled with respect to the Cartesian coordinates of $\vec{A}$ according to (19). This allows replacement of the nonlinear vector problem by a series of linear scalar problems with changing right hand sides. The matrix remains constant during iteration and has therefore to be assembled and factorized only once. The convergence rate can be improved by applying an adaptive relaxation technique [4]. The numerical example described in the next section has been treated with $M(B)$-iteration.

V. Numerical Example

The numerical behaviour of the BEM-FEM coupled methods has been studied using TEAM workshop problem 13 [8]. Problem 13 consists of two steel channels around a coil with either 3000 AT or 1000 AT DC excitation and a steel center plate, Fig. 2. Taking advantage of the symmetry, only 1/4 of the problem region had to be discretized. The steel parts have been treated with 20-noded quadratic finite elements. The interface between steel and air coincides with the coupling boundary $\Gamma_{\mathrm{BEM}} = \Gamma_{\mathrm{FEM}}$ and has been meshed with 8-noded quadratic boundary elements. Additional 20-noded quadratic volume elements have been used for the representation of the exciting current in the domain Ω_{BEM}. The mesh structure is shown in Fig. 3 and some discretization data are given in Table I. To determine the accuracy of the calculations, a comparison with measured flux densities given in [8] for certain positions in the steel parts and in the air has been performed, Fig. 4. Fig. 5 shows the results. It turned out that both formulations behave practically identically and that the computed results are in good agreement with the measured ones, especially for the 3000 AT excitation in steel and for 1000 AT in the air.

The TEAM workshop problem 10, which is very similar to problem 13, was studied under DC conditions in [9].

TABLE I
Mesh Data For Problem 13

Number of nodes in steel	7391
Number of FEM elements	1200
Number of BEM elements	1398
Number of nodes in the air	3984
Number of volume BEM elements	700
Total number of equations	21087

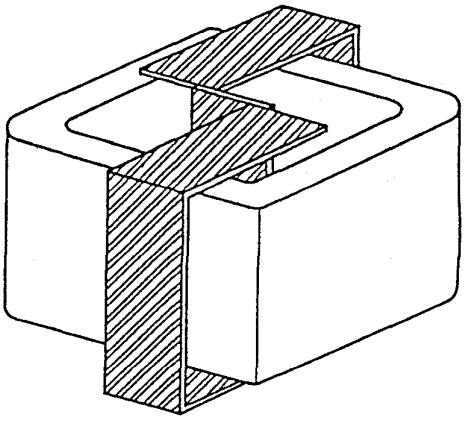

Fig. 2. TEAM workshop problem 13

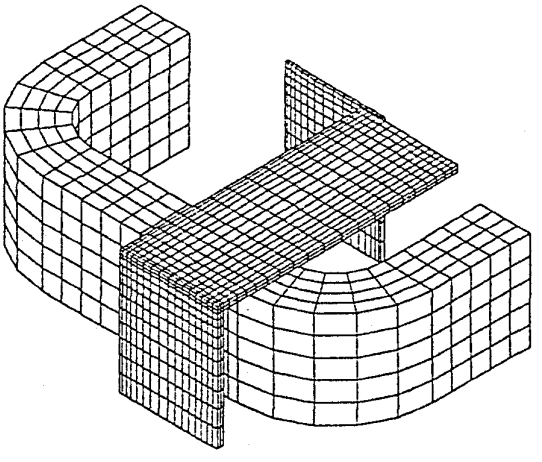

Fig. 3. Discretization of problem 13

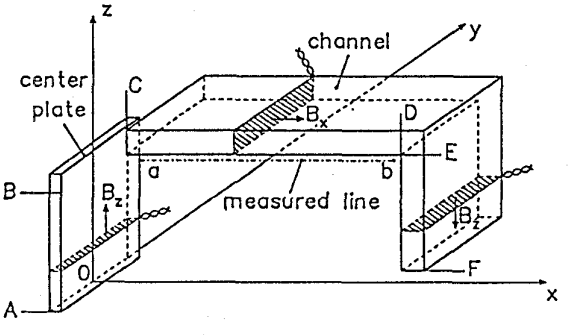

Fig. 4. Specified positions for comparing average flux densities in steel along the lines A–B (B_z), C–D (B_x), E–F (B_z) and flux density in the air along the line a–b ($|\vec{B}|$).

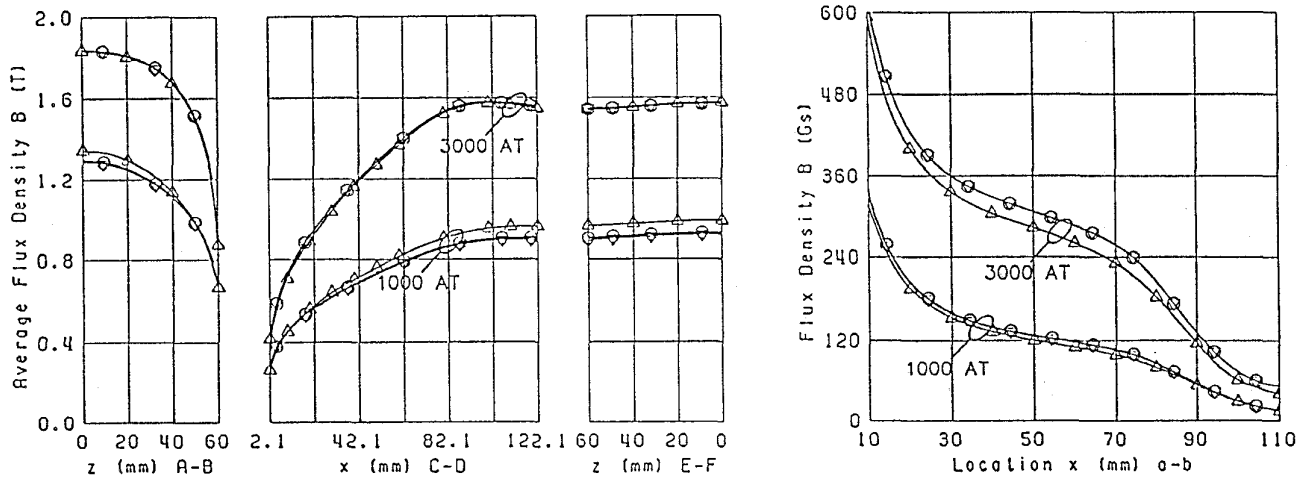

Fig. 5. Comparison between measured and computed results
△ Measured, O 1st Formulation, ▽ 2nd Formulation

It was reported that the formulation (5) using finite elements only led to accuracy problems on iron/air interfaces, which could be overcome by introducing additional degrees of freedom for A_n. In our calculation, the iron/air interface is identical with the BEM-FEM coupling boundary. To allow direct comparison with [9], the distribution of the flux density along the line $x = 0$, $z = 0$ has been examined, Fig. 6.

In the case of 1000 AT, the flux density begins to decrease at $y = 18$ mm and attains even negative values in the vicinity of the interface. For that reason, the average flux density within the steel plates (Fig. 5) is slightly too small. Our experiments showed, that simple mesh refinement does not improve the accuracy very much. It seems that the behaviour of the BEM-FEM coupling at the iron/air interface is very much the same as with finite elements only. Further investigations have to be carried out to confirm this assumption and to overcome the numerical difficulties.

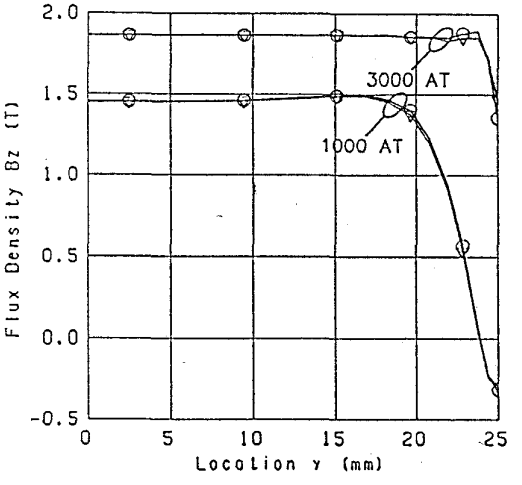

Fig. 6. Distribution of the flux density in the center plate along the line $x = 0$, $z = 0$: O 1st Formulation, ▽ 2nd Formulation

References

[1] O. Biro and K. Preis, "On the use of the magnetic vector potential in the analysis of 3-dim. eddy currents," *IEEE Transactions on Magnetics*, vol. 25(4), pp. 3145–3159, July 1989.

[2] E. Schlemmer, J. Steffan, W.M. Rucker and K.R. Richter, "Accuracy improvement using a modified Gauss-quadrature for integral methods in electromagnetics," *IEEE Transactions on Magnetics*, vol. 28(2), pp. 1755–1758, March 1992.

[3] K.D. Paulsen and D.R. Lynch, "Elimination of vector parasites in finite element Maxwell solutions," *IEEE Transactions on Microwave Theory and Techniques*, vol. 39(3), pp. 395–404, March 1991.

[4] S. Kurz, J. Fetzer and G. Lehner, "Comparison between different iterative methods for calculation of magnetostatic fields in nonlinear media," *Proc. of the 6th International IGTE Symposium*, Graz, Austria, pp. 77–82, 1994.

[5] B.B. Shyamkumar and Z.J. Cendes, "Convergence of iterative methods for nonlinear magnetic field problems," *IEEE Transactions on Magnetics*, vol. 24(6), pp. 2585–2587, November 1988.

[6] Y. Kanai, T. Abe, M. Iizuka and K. Mukasa, "Fast and stable non-linear converging method," *IEEE Transactions on Magnetics*, vol. 23(5), pp. 3290–3292, September 1987.

[7] D.S. Bloomberg and V. Castelli, "Reformulation of nonlinear magnetostatic equations for rapid iterative convergence," *IEEE Transactions on Magnetics*, vol. 21(2), pp. 1174–1180, March 1985.

[8] T. Nakata, N. Takahashi and K. Fujiwara, "Summary of results for TEAM workshop problem 13 (3-D nonlinear magnetostatic model)," *Proc. of the 4th international TEAM workshop*, Miami, Florida, pp. 33–39, 1994.

[9] K. Preis et.al., "Numerical analysis of 3D magnetostatic fields," *IEEE Transactions on Magnetics*, vol. 27(5), pp. 3798–3803, September 1991.